

Compressed Sensing for Faster Optical-resolution Photoacoustic Microscopy: A Simulation Framework

I Gede Eka Sulistyawan^{1‡}, Daisuke Nishimae², Takuro Ishii^{1,3}, and Yoshifumi Saijo¹
(¹Grad. School of Biomed Eng, Tohoku Univ.; ²School of Eng., Tohoku Univ.; ³FRIS, Tohoku Univ.)

1. Introduction

Optical resolution photoacoustic microscopy (OR-PAM) has been developed to visualize microvascular with high spatial resolution. In general, the OR-PAM system requires to scan the target point-by-point by moving the opt-acoustic probe in two orthogonal directions. In the early development of OR-PAM, the scanning was done using linear stages, but the linear scanning had a limited imaging speed. To improve the system, later studies have investigated the utilization of micro-electromechanical system (MEMS) mirrors that translates the linear movement into the rotational movement and thus might increase the imaging speed of OR-PAM. A study used a combination of single direction MEMS and linear stage¹⁾, while another group developed a dual-direction MEMS²⁾. In addition, a polygon mirror was employed as substitute to the MEMS³⁾. Those attempts have proven the efficacy of the MEMS in improving the speed of the OR-PAM, however the improved speed is still in a range of 8 – 400 seconds for $1 \times 1 \text{ cm}^2$, which is insufficient to visualize temporal changes such as intra-cellular biochemical interactions and minute hemodynamics.

A potential solution is reducing the number of sampling point, in addition to using the MEMSs' fast scanning technique, and decreasing the acquisition time. To do so, an emerging technique called compressed sensing (CS) may be used to reconstruct the full resolution image data from the under sampled scanning point. This study investigates the applicability of CS in an OR-PAM system equipped with a single-direction MEMS mirror and a single-direction linear stage by simulating an under-sampling condition.

2. Material and Methods

2.1 Experiment setup and data acquisition

The OR-PAM system comprised of a single-axis waterproof MEMS (1A-WP-MEMS) and a linear stage¹⁾. The object was illuminated with focused laser (Wavelength: 532 nm, Pulse repetition frequency (PRF): 10 kHz), and the yielded photoacoustic signal was captured with an unfocused ultrasound (Center frequency: 50 MHz, Frequency sampling: 500 MS/s).

A black-stained leaf skeleton phantom was chosen as the experiment object. The dimension of the imaging was a patch of $2 \text{ mm} \times 2 \text{ mm}$ and a depth of 0.75 mm. The speed of the linear stage was dependent on the MEMS and pulse repetition frequency (PRF). Following this setup¹⁾, the linear stage speed was $62 \mu\text{m/s}$ and able to obtain full resolution scanning in 32 seconds.

2.2 Signal processing

The acquired radio frequency data was band-pass filtered (5 – 100 MHz) then Hilbert transformed (HT). The OR-PAM system requires distortion correction as the motion of the MEMS mirror introduces linear and non-linear distortions in the polar axis¹⁾. Once corrected, a Maximum Intensity Projection (MIP) image was obtained by normalizing and picking the maximum amplitude of each HT data. An illustration shown in **Fig. 1 (a)** and the yielded MIP image for ground-truth was shown in **Fig. 1 (b)**.

2.3 Sampling simulation

A CS framework was devised to generate a full-resolution MIP image from an under-sampled dataset. Although the CS framework requires an acquisition dataset randomly sampled over the 2D imaging field, performing randomization was considered in obstructing the advantage of resonant movement of the MEMS. To achieve both minimum sampling and retain the resonant movement of MEMS, a simulation was done by increasing the speed of the linear stage.

Considering the original linear stage speed was $62.5 \mu\text{m/s}$, the simulated samplings were performed on $188 \mu\text{m/s}$, $250 \mu\text{m/s}$ and $383 \mu\text{m/s}$ for 12.8 seconds. These speeds were approximately 3, 4 and 6 times faster than the original. The under-sampled data obtained from simulation was shown in **Fig. 1 (c – e)**. These data then transferred into the CS reconstruction that is described in the next section.

2.4 Reconstruction

Consider a reconstruction of a full resolution MIP image $M \in \mathbb{R}^{m \times n}$ from an obtained under-sampled data $Y \in \mathbb{R}^{p \times 1}$ with $p \ll mn$. To match the dimension, a vectorized $M \in \mathbb{R}^{mn \times 1}$ was used

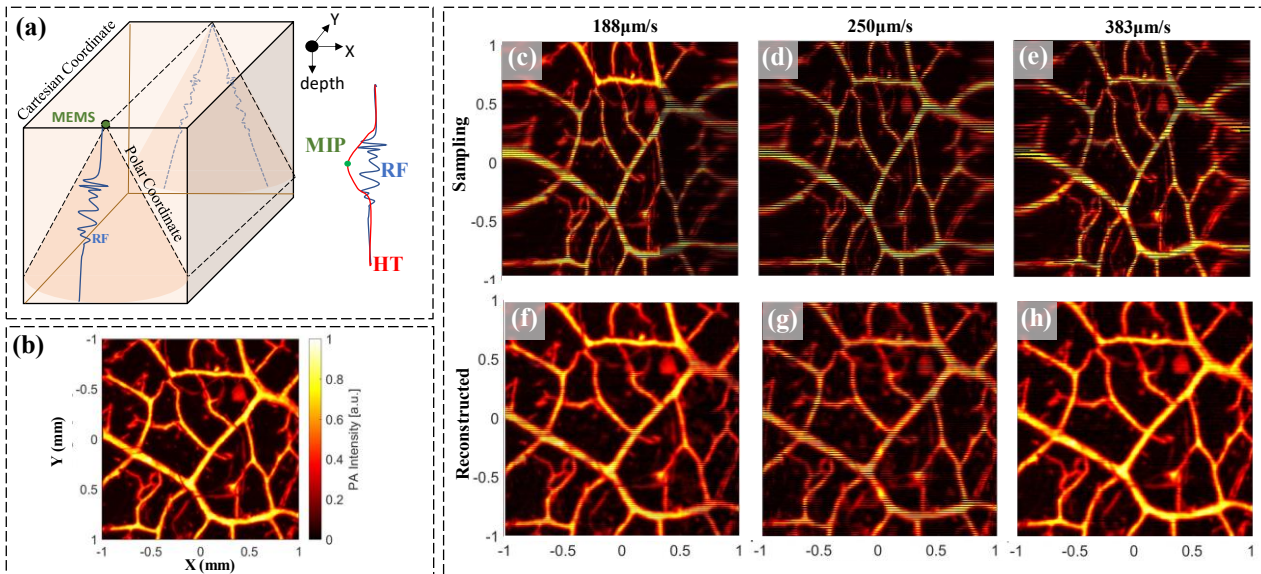


Fig. 1. (a) Acquisition in polar coordinate. (b) Ground-truth. (c-h) Under sampling simulation on various linear stage speed for 12.8 seconds. (c, d, e) Sampling pattern. (f, g, h) reconstructed MIP after minimization and distortion correction.

instead. The process of a CS reconstruction was to iteratively estimate M closer to Y with a prior knowledge on the sparsity of M . To achieve the goal, Y was modeled as sampling M with pattern $C \in \mathbb{Z}^{p \times mn}$, i.e., $Y = CM$. Then, an Inverse Discrete Cosine Transform (IDCT) $\Psi \in \mathbb{R}^{mn \times mn}$ was used to obtain M from its sparse representation $X \in \mathbb{R}^{mn \times 1}$, i.e., $M = \Psi X$. Finally, the reconstruction algorithm can be represented in the following equation,

$$\min_X \|C\Psi X - Y\|_2^2 + \|X\|_1 \quad (1)$$

A Sub-gradient algorithm was utilized to solve Equation 1. The obtained reconstructed MIP image then distortion corrected before evaluation. Evaluation was done using Structural Similarity (SSIM)⁴ and Mean Squared Error (MSE) against the ground-truth.

3. Results and discussion

The reconstructed full resolution images were shown in Fig. 1 (f – h). The yielded images were similar with the ground-truth, implying the success of the algorithm to reconstruct the data. Nevertheless, artifacts still existed in some parts of the images. Structurally, the artifact was similar to the scanning pattern. This suggests that the artifact might be originated from the scanning pattern.

A quantitative evaluation was shown in **Table 1**. The best and worst performance was achieved by the speed 383 $\mu\text{m/s}$ and 250 $\mu\text{m/s}$, respectively. With simulation that allows backward

Table 1. SSIM and MSE for different stage speeds compared to ground-truth.

	188 $\mu\text{m/s}$	250 $\mu\text{m/s}$	383 $\mu\text{m/s}$
SSIM	0.486	0.253	0.642
MSE	0.009	0.026	0.002

scanning for more scanning points, increasing speed should be associated with increasing performance. However, there exist speeds (e.g., 250 $\mu\text{m/s}$) that had the same path while scanning backward. This causing in unimproved scanning points, thus limits the reconstruction algorithm and should be avoided.

The current study utilized Sub-gradient algorithm without considering the undifferentiable properties of the Equation 1. This motivates further investigation to different algorithm that able to overcome this limitation. In addition, an identification of the origin of the artifact might help in guiding to a better problem formulation, rather than relying only on sparsity. In the future, it is interesting to modify Equation 1 to suppress the artifact.

4. Conclusion

In this paper, the applicability of CS framework on OR-PAM with 1-axis MEMS and a linear stage had investigated. Despite of under controlled simulation, the experiment results showed positive potentials of the CS implementation in the real system that will significantly increase the imaging acquisition time.

References

1. R. Shintate, T. Ishii, J. Ahn, J. Y. Kim, C. Kim, and Y. Saijo: Sci. Rep. **12** (2022) 9221.
2. J. Y. Kim, C. Lee, K. Park, G. Lim, and C. Kim: Sci. Rep. **5** (2015) 7932.
3. B. Lan, W. Liu, Y. Wang, J. Shi, Y. Li, S. Xu, H. Sheng, Q. Zhou, J. Zou, U. Hoffmann, W. Yang, J. Yao: Biomed. Opt. Express **9** (2018) 4689.
4. Z. Wang, A. C. Bovik, H. R. Sheikh, E. P. Simoncelli: IEEE Trans. Image Process. **13** (2004) 600.